

# Quantum Zeno subspace and entangled Bose-Einstein condensates

M. Zhang<sup>1,\*</sup> and L. You<sup>1,2</sup>

<sup>1</sup>School of Physics, Georgia Institute of Technology, Atlanta, Georgia 30332, USA

<sup>2</sup>Interdisciplinary Center of Theoretical Studies and Institute of Theoretical Physics, CAS, Beijing 100080, China  
(April 14, 2024)

We discuss a proposal for the efficient generation of the maximally entangled atomic N-GHZ state in a spinor-1 condensate by driving internal state atomic Raman transitions using (classical) laser fields. We illustrate the dynamics in terms of a quantum Zeno subspace, and identify the resultant atomic elastic collision in facilitating the deterministic entanglement creation. Our proposal can be readily implemented in several laboratories where ferromagnetic spinor condensates (of  $^{87}\text{Rb}$  atoms) are investigated.

03.65.Xp, 03.67.Mn, 03.75.Gg, 03.75.Mn

The continued success of the research on quantum degenerate atomic gases has led to intense exploration of their potential application for quantum information science. A substantial topic of recent interest is the creation of spin-squeezed atomic states that display multiparticle inseparable correlations [1,2]. While it is debatable how such inseparable quantum correlations among identical particles are related to entanglement between distinct parties [3,4], it has nevertheless been fruitful to investigate these unexplored territories. Maximally entangled states enjoy special attention; in addition to being states of maximum inseparable correlations or entanglement, they compose of a special class with which theoretical discussions can become most transparent.

Recently, a deterministic protocol was suggested [5] for creating maximally entangled pairs, triplets, quartets, and other clusters of Bose condensed atoms starting from a condensate in the Mott insulator state [6]. The work of [5] concerns a single optical well and involved a small number of atoms. In this limit, the evolution dynamics of the system is analytically solvable, which allows the appropriate timing of the external laser fields (in comparison with atom elastic collision strength) to be identified for creating maximal atomic entanglement.

This article clarifies the operating mechanism of the seemingly simple protocol [5]. More importantly, we investigate its application to large numbers of condensed atoms. To our surprise, the few atom protocol with classical laser fields driving atomic Raman transitions remains efficient in generating massive atomic entanglement of condensed atoms. The answer, it turns out, can be obtained rather conveniently understood in terms of a quantum Zeno subspace [7]. Within this subspace, the effective atom interaction and the Raman dynamics reduces to a well-known form studied earlier [8]. What is crucial for creating maximally entangled atomic states is

to start from a condensate with a fixed number of atoms, (be it even or odd [8]).

This paper is organized as follows. First, we briefly introduce our system and the setup for generating maximal entangled atomic states. Then we provide a step by step illustration of the underlying mechanism for the creation of such massively correlated atomic states. We briefly review the concept of a quantum Zeno subspace [7]. This is followed by a review of a spin-1 condensate, paying special attention to the case of ferromagnetic atom-atom interactions (as for  $^{87}\text{Rb}$  atoms). We then discuss an interesting decomposition of the interaction Hamiltonian into three sub-SU(2) spaces as first suggested in [9]. Finally, we show that the external laser fields in the appropriate Raman configuration create a quantum Zeno subspace, within which the effective interaction is of the desired form for generating spin squeezing and maximal atomic entanglement. We conclude with some illustrative numerical results.

Our main result can be summarized in Fig. 1 below. We consider a spin-1 ( $F = 1$  atoms with three Zeeman sub-levels) condensate with a fixed number ( $N$ ) of atoms that are all in the  $|j=1, m_F=1\rangle$  or  $|j=1, m_F=-1\rangle$  state initially. We claim that if a strong off-resonant Raman transition is established between the  $|j=1, m_F=1\rangle$  and  $|j=1, m_F=-1\rangle$  state, then at predictable instants of the time evolution, the condensate becomes maximally entangled, i.e. its atomic internal state becomes an  $N$ -atom GHZ state  $|j=1, m_F=1\rangle^N + |j=1, m_F=-1\rangle^N$ .

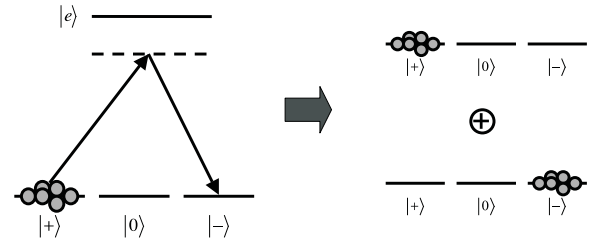


FIG. 1. Illustration of our basic result.

**Quantum Zeno subspace** The quantum measurement process itself can strongly affect the dynamics of a system. An often cited example in this regard is the famous quantum Zeno effect [10,11]: a watched pot does not boil, or in a physical system, frequent measurements of the initial state hinders its dynamics to evolve to other states. Recently, Facchi and Pascazio provided new insights into the Zeno effect, by reformulating it in terms

of an adiabatic theorem within different sectors of the so-called quantum Zeno subspaces [7], which are closely related to the powerful decoherence free subspace in quantum computing studies [12,13]. In terms of the notation of [7], the concept of a quantum Zeno subspace can be illustrated by a system Hamiltonian

$$H = H + H_{\text{meas}}; \quad (1)$$

In the limit of an infinitely large parameter  $\lambda$ , the time evolution of  $H$  is diagonal with respect to spaces of  $H_{\text{meas}}$ , i.e. for any Hamiltonian of the form (1), the largest term  $H_{\text{meas}}$  decomposes the complete Hilbert space into different subspaces or quantum Zeno subspaces. The dynamics associated with the small term  $H$  is slowed to slow adiabatic evolutions within each of these orthogonal subspaces.

**Spinor condensate** For ferromagnetic interactions (e.g.  $^{87}\text{Rb}$ ), as was shown before [14], the spatial mode of different condensate component  $\psi_j(\mathbf{r})$  (normalized to unity) is identically the same  $\psi(\mathbf{r})$ . Thus, a spin-1 condensate can be described with  $a_{j=+;0}$ ;  $(a_{j=+;0}^\dagger)$ , the single atom annihilation (creation) operator for each spin component state. Apart from constant terms that depend on the total number of atoms  $N = N_+ + N_0 + N_-$ , ( $N_j = a_{j=+;0}^\dagger a_{j=+;0}$ ), the atom-atom interaction becomes [15][17]

$$H = uL^2; \quad (2)$$

where the coefficient is  $u = c_2 \int d\mathbf{r} \psi^\dagger(\mathbf{r}) \psi(\mathbf{r}) \psi^\dagger(\mathbf{r}) \psi(\mathbf{r}) = 2(u < 0 \text{ for ferromagnetic interactions})$ .  $c_2 = 4\hbar^2(a_2 - a_0)/3M$  with  $a_2$  and  $a_0$  the respective scattering lengths in the total spin  $F = 2$  and 0 channels of two colliding spin-1 atoms. The pseudo angular momentum operator  $L$  is defined according to the Schwinger representation, and with its components given by

$$\begin{aligned} L_+ &= L_x + iL_y = \frac{1}{2}(a_+^\dagger a_0 + a_0^\dagger a_+); \\ L_- &= L_x - iL_y = \frac{1}{2}(a_+^\dagger a_+ - a_0^\dagger a_0); \end{aligned} \quad (3)$$

It is well known [9] that such an effective interaction (2) is formally SU(2) symmetric, thus would have not generated any nonlinear dynamics if the  $L_j$ 's were the SU(2) Schwinger representation of two bosonic modes [18]. For the spin-1 condensate being considered here, as was emphasized before [9], the pseudo angular momentum operator  $L$  does NOT satisfy the Casimir relation  $[L^2 \notin N(N+1)]$ , and therefore can not really be considered an angular momentum operator [9]. Using the Gell-Mann decomposition of SU(3) into three SU(2) subspaces  $U$ ,  $V$ , and  $T$ , it was found [9] that

$$L^2 = 4T_z^2 + 2(V_+ U_+ + V_- U_-) + (N_+ - N_-)(N_+ + N_-) = 2(N_+^2 - N_-^2); \quad (4)$$

with  $N_\pm = \frac{1}{2}(N \pm 3)$  and  $Y_0 = N = 6$ ,  $1 = 4$ . It is important to note that operators belonging to different

SU(2) subspaces do not always commute. We adopt the convention that

$$T_+ = a_+^\dagger a_-; \quad T_z = \frac{1}{2}(a_+^\dagger a_+ - a_-^\dagger a_-); \quad (5)$$

$$\begin{aligned} V_+ &= a_+^\dagger a_0; & V_z &= \frac{1}{2}(a_+^\dagger a_+ + a_0^\dagger a_0); \\ U_+ &= a_+^\dagger a_0; & U_z &= \frac{1}{2}(a_+^\dagger a_+ - a_0^\dagger a_0); \end{aligned} \quad (6)$$

and the hypercharge  $Y = (N_+ + N_- - 2N_0)/3$ , which physically corresponds to the quadrupole moment of atomic populations  $N_{j=+;0}$ .

**Effective interaction and maximal entanglement generation** A Hamiltonian of the form  $T_z^2$  [the first term in Eq. (4)] can be used to generate maximally entangled or spin squeezed states [12,8,19]. To selectively suppress other terms in the Hamiltonian Eq. (2), we resort to the idea of quantum Zeno subspace as reviewed earlier. In this case, to limit the dynamics to the manifold composed of internal states  $|j \uparrow i$  and  $|j \downarrow i$ , we simply Raman couple them with strong external laser fields, in the form  $(T_+ - T_-) = 2i = T_y$  as shown in Fig. 1. In the spirit of the adiabatic theorem within the Zeno subspace [7], our system dynamics is now governed by

$$H^0 = 4uT_z^2 + T_y; \quad (7)$$

an effective Hamiltonian that is known to generate maximally entangled states [5,8].

The shortest time for creating a maximally entangled state when initially all atoms are in either  $|j \uparrow i$  or  $|j \downarrow i$  is,  $\tau = 4\pi\hbar/J$  a factor of two longer than that from a bare interaction of the form  $H^0 = 4uT_x^2$  [5]. This point becomes clear when we transfer to the interaction picture  $j(t)i_I = \exp(iT_y t)j(t)i$  as now  $T_y$  becomes the largest term in the system Hamiltonian. Equation (7) arises when the limit  $N \gg j$  is satisfied. The effective Hamiltonian in the interaction picture then becomes

$$\begin{aligned} H_{\text{int}}^0 &= e^{i T_y t} (4uT_z^2) e^{-i T_y t} \\ &= 4u(T_z \cos t - T_x \sin t)^2 \\ &\quad - 2u(T_z^2 + T_x^2) = 2uT^2 - 2uT_y^2; \end{aligned} \quad (8)$$

where the approximation is due to averaging over the rapid Rabi oscillations. The first term  $\propto T^2$  in Eq. (8) is SU(2) symmetric in the two dimensional subspace of  $|j \uparrow i$  and  $|j \downarrow i$ , thus it can be neglected as it only introduces an overall phase factor. The second term,  $\propto T_y^2$  (with a coefficient a factor of 2 smaller), is similar to the  $T_x^2$  term [5,8], thus explaining the dynamic creation of maximally entangled states. The entanglement remains for the Schrodinger picture based atomic states as the two pictures coincide at integer periods of the Rabi oscillation. The rapid time average results in a factor of two reduction of the effective interaction strength.

We now present selective results from numerical simulations based on the complete Hamiltonian (2) plus the Raman term  $T_y$  and compare with the approximate results based on the adiabatic Hamiltonian (7).

Figure 2 demonstrates the validity of a quantum Zeno subspace ( $|j \uparrow i\rangle$  and  $|j \downarrow i\rangle$ ) with increasing values of the effective Rabi frequency and for two different atom numbers. Indeed, when  $\Omega$  becomes larger as compared to  $N|j \downarrow j\rangle$ , the populations become increasingly localized within the isospin subspace ( $|j \uparrow i\rangle, |j \downarrow i\rangle$ ), and eventually the Hamiltonian  $H^0$  correctly describes the dynamics and maximally entangled N-GHZ states are created at  $t = \pi/4|j \downarrow j\rangle$ . The creation of a Zeno subspace can be further illustrated by watching the time dependent population distributions as in Figs. 3 and 4.

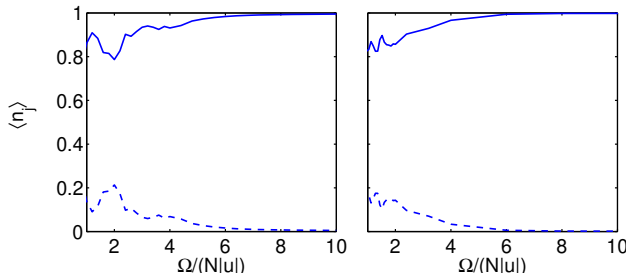


FIG. 2. The average fraction of atoms in the Zeno subspace  $n_z = \langle N_{+} + N_{-} \rangle / N$  (solid line) and in state  $|j \downarrow i\rangle$ ,  $n_0 = \langle N_0 \rangle / N$  (dashed line) for  $N = 10$  (left panel) and 50 (right panel) at  $t = \pi/4|j \downarrow j\rangle = 5$  (ms). The qualitative dependence is similar at other times.  $u = (2\pi) = 25$  (Hz) and initially all atoms in state  $|j \uparrow i\rangle$ .

We found that if a strong Raman coupling is established between states  $|j \uparrow i\rangle$  ( $|j \downarrow i\rangle$ ) and  $|j \downarrow i\rangle$ , a quantum Zeno subspace composed of atoms in these two states is also created. However, maximally entangled states do not occur as the projection of  $L^2$  into this space does not yield the required nonlinear interaction  $V_z^2$  ( $U_z^2$ ) [9].

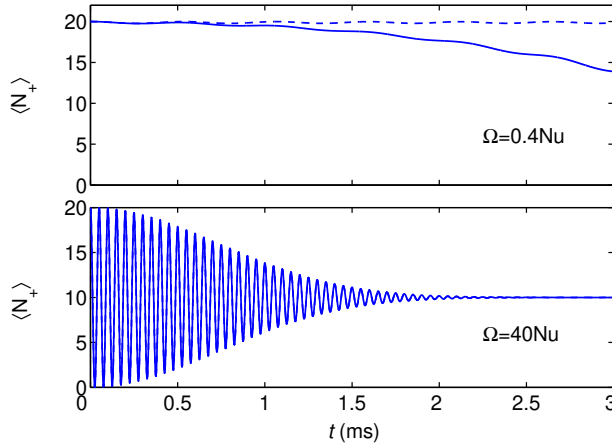


FIG. 3. The time dependence of  $\langle N_{+} \rangle$  for  $N = 20$ ,  $u = (2\pi) = 25$  (Hz), and initially all atoms in state  $|j \uparrow i\rangle$ . The solid line is from the complete Hamiltonian while the dashed line is from the adiabatic Hamiltonian in the Zeno subspace. At  $t = 40N|j \downarrow j\rangle = 40$  ( $20N|j \downarrow j\rangle = (2\pi)20$  (kHz) (lower panel), the Zeno subspace is well established.

We now discuss the generation of N-GHZ states when

$N|j \downarrow j\rangle$ . Because the interaction picture Hamiltonian (8) is similar to that of Molmer's model as in [8], we anticipate similar dynamical behaviors. We adopt the notion of the maximal entangled fraction and define the optimized overlap

$$F_{\max} = \max_{|j \downarrow j\rangle} \langle j \downarrow j | H^0 | j \downarrow j \rangle = 0.5(|j \downarrow j\rangle + |j \uparrow j\rangle)^2; \quad (9)$$

of the N-atom wave function  $|j \downarrow j\rangle(t)$  with an entangled coherent spin state [20]

$$|j \downarrow j\rangle = \frac{1}{\sqrt{2}}(|j \downarrow j\rangle + e^{i\phi}|j \uparrow j\rangle); \quad (10)$$

with  $\phi = \arg(\langle j \downarrow j | H^0 | j \downarrow j \rangle) + \arg(\langle j \uparrow j | H^0 | j \uparrow j \rangle)$ . For  $F_{\max}$  we note  $\phi = \arg(\langle j \downarrow j | H^0 | j \downarrow j \rangle) - \arg(\langle j \uparrow j | H^0 | j \uparrow j \rangle)$ .

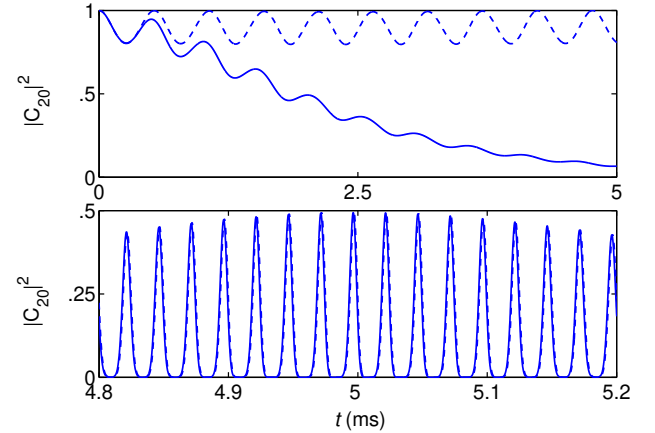


FIG. 4. The same as in Fig. 3 but the probability for all atoms in  $|j \downarrow i\rangle$ .  $C_N = \langle j \downarrow j | H^0 | j \downarrow j \rangle / N!$ . Note the creation of a N-GHZ state at time  $t = 5$  (ms) (lower panel).

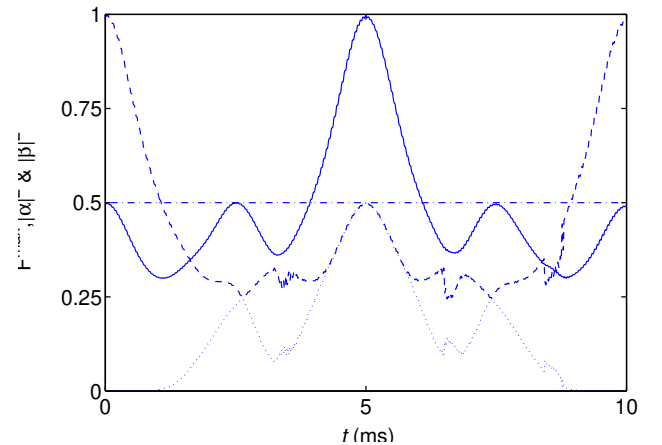


FIG. 5. The time dependence of  $F_{\max}$  (solid line),  $|j \downarrow j\rangle$  (dashed line), and  $|j \uparrow j\rangle$  (dotted line) for  $N = 20$ ,  $u = (2\pi) = 25$  (Hz), and  $\Omega = (2\pi)10$  (kHz).

In Fig. 5, we display the time dependence of  $F_{\max}$  with the use of the adiabatic Hamiltonian (7). We see two interesting regimes. For times up to  $t = (N/2)\tau$ , the wave function is almost a coherent spin state, so the mean field theory can be used to describe the system dynamics [19]. Around  $t = (N/2)\tau = 5$  (in units), however, we obtain a highly entangled coherent spin state, where the mean field theory completely breaks down. We also find that the angles  $\theta_{\max}$ ,  $\phi_{\max}$ , and  $\chi_{\max}$  are essentially constant in the immediate neighborhood of  $t = (N/2)\tau = 5$  (in the interaction picture), thus a phase sensitive detection of the massive entanglement can be accomplished without extremely precise timing [19,21].  $F_{\max}$  has been proven to be a useful measure of  $N$ -atom entanglement: a  $N$ -atom pure state  $|j\rangle$  is entangled if  $F_{\max} > 1/2$  (above the dash dotted line in Fig. 5) [22,23].

Finally, we note that the maximally entangled state  $|j\rangle^N + |j\rangle^N$  as generated with our method is stable against elastic two body collisions, thus is ideal for studying multiple atom entanglement. Furthermore, our protocol works, even when there is a non-zero magnetic field that breaks the level degeneracy for different spin components. The Zeeman interaction gives rise to

$$H_B = \hbar \omega_L (a_+^\dagger a_+ - a_-^\dagger a_-) + \hbar (a_+^\dagger a_+ + a_-^\dagger a_-); \quad (11)$$

where the linear Zeeman term is proportional to the Larmor precessing frequency  $\omega_L = B_B/\hbar$ , with  $B_B$  the magnetic dipole moment for state  $|j\rangle$ , and the quadratic term is proportional to  $\omega_L^2/B^2$ , one half the energy released from the generation of two atoms in state  $|j\rangle$  due to the elastic collision of one atom in state  $|j\rangle$  with another one in state  $|j\rangle$ . In the quantum Zeno subspace,  $a_+^\dagger a_+ + a_-^\dagger a_- = N$ , remains a constant, so the quadratic Zeeman term does not affect the dynamics of generating maximally entangled  $N$ -GHZ states. The linear Zeeman term is  $\propto T_z$ , which simply induces a twisted phase on the state  $|j\rangle$ . In the rotating frame, the atom-atom interaction term remains the same  $4uT_z^2$ , while the Raman coupling  $T_y$  now contains time dependent phase factors  $e^{\pm i\omega_L t}$ . Nevertheless the complete system dynamics remain the same. Therefore we expect our theoretical protocol to remain effective.

In conclusion, we have proposed a protocol for robustly generating maximally entangled atomic states in a condensate. We have illuminated the operating principle in terms of a quantum Zeno subspace. Our protocol can be implemented in currently available condensate systems with ferromagnetic interactions, where the spatial mode functions are identical for each of the components [14]. It can also be applied to spin-1 condensates with anti-ferromagnetic interactions (e.g.  $^{23}\text{Na}$  atoms [24]), which may possess larger values of exchange interaction  $u$ , thus leading to faster generation of entangled condensates. Although the different equilibrium mode functions in the latter case can lead to modulational instability, thus increased decoherence of the maximally entangled state [14]. Our protocol starts with all condensed atoms

in either state  $|j\rangle$  or  $|j\rangle$ . Provided the time scale  $1/\omega_L$  is reasonably short as compared to the inverse of a typical condensate phonon frequency, the dynamics for generating entangled condensate is also mechanically stable, irrespective of whether the  $|j\rangle$  or  $|j\rangle$  condensate component is miscible (for anti-ferromagnetic interactions) or not (ferromagnetic interactions).

This work is supported by NSF, CNSF, and by a grant from NSA, ARDA, and DARPA under ARO Contract No. DAAD19-01-1-0667.

---

<sup>y</sup> Current address: Center for Advanced Study, Tsinghua University, Beijing, 100084, China.

- [1] A. Sørensen, L.-M. Duan, J. I. Cirac, and P. Zoller, *Nature* 409, 63 (2001), and references therein.
- [2] Kristian Helmerson and L. You, *Phys. Rev. Lett.* 87, 170402 (2001).
- [3] R. Paskauskas and L. You, *Phys. Rev. A* 64, 042310 (2001); Y. S. Li et al., *ibid.*, 054302 (2001); J. Schliemann et al., *ibid.*, 022303 (2001).
- [4] Andrew P. Hines et al., *Phys. Rev. A* 67, 013609 (2003).
- [5] L. You, *Phys. Rev. Lett.* 90, 030402 (2003).
- [6] M. Greiner et al., *Nature* 415, 39 (2002).
- [7] P. Facchi and S. Pascazio, *Phys. Rev. Lett.* 89, 080401 (2002).
- [8] K. Mølmer and A. Sørensen, *Phys. Rev. Lett.* 82, 1835 (1999).
- [9] O. Mestechaplov et al., *Phys. Rev. A* 66, 033611 (2002).
- [10] R. J. Cook, *Phys. Scr. T* 21, 49 (1988).
- [11] W. M. Itano et al., *Phys. Rev. A* 41, 2295 (1990).
- [12] A. Beige et al., *Phys. Rev. Lett.* 85, 1762 (2000).
- [13] D. A. Lidar et al., *Phys. Rev. Lett.* 81, 2594 (1998).
- [14] S. Y. Lee et al., *Phys. Rev. A* 66, 011601 (2002).
- [15] C. K. Law et al., *Phys. Rev. Lett.* 81, 5257 (1998); H. Pu et al., *Physica B* 280, 27 (2000).
- [16] T.-L. Ho and S. K. Yip, *Phys. Rev. Lett.* 84, 4031 (2000).
- [17] M. Koashi and M. Ueda, *Phys. Rev. Lett.* 84, 1066 (2000).
- [18] M. Kitagawa and M. Ueda, *Phys. Rev. Lett.* 67, 1852 (1991).
- [19] A. M. Icheli, D. Jaksch, J. I. Cirac, and P. Zoller, *Phys. Rev. A* 67, 013607 (2003), and references therein.
- [20] As in Ref. [18],  $|j\rangle = (\cos \frac{\theta}{2} a_+^\dagger + e^{i\phi} \sin \frac{\theta}{2} a_-^\dagger) |j\rangle$ .
- [21] M. Zhang, K. Helmerson, and L. You, *Phys. Rev. A* (in press); (cond-mat/0212286).
- [22] Xiaoguang Wang et al., *Phys. Rev. A* 67, 022302 (2003); C. A. Sackett et al., *Nature (London)* 404, 256 (2000); M. Seevinck and J. Uink, *Phys. Rev. A* 65, 012107 (2002); J. Uink, *Phys. Rev. Lett.* 88, 230406 (2002).
- [23] B. Zeng et al., *Phys. Rev. A*, (in press).
- [24] J. Stenger et al., *Nature* 396, 345 (1998).